Geometrical Structure of Yttrium and Metal–Bromine Complexes in Solution: Limitations of Extended X-ray Absorption Fine Structure Analysis (EXAFS)

Jesús Chaboy,*[a] Adela Muñoz-Páez,[b] and Sofía Díaz-Moreno[c]

Abstract: An extensive study on the appearance of multi-electron features in the X-ray absorption spectra of several yttrium(III)-based compounds has been performed. The existence of a multi-electron transition of non-negligible intensity within the extended X-ray absorption fine structure (EXAFS) region of the Y K-edge spectra has been proven. The impact of such features in the EXAFS analysis is made evident for aqueous solutions of $YBr_3 \cdot 6H_2O$ in liquid and glassy states in the concentration range 0.005–2.0 M, in which this transition induces an overestimation in the coordination numbers derived from EXAFS. We have performed theoretical computation of cross-sections for the double-electron processes at the K-edge of both Y and Br. These computations have been applied to the experimental EXAFS K-edge spectra of both Y and Br in several solids and in aqueous solutions. While in the case of Y K-edge spectra the presence of such multi-electron transitions was seen to seriously affect the standard EXAFS analysis, its influence in the case of Br K-edge spectra was determined to be negligible.

Keywords: bromine · EXAFS spectroscopy · structure elucidation · yttrium

Introduction

The determination of the geometrical structure of solutions of metal complexes is indispensable for the understanding of their chemical behaviour. In order to describe the complexation behaviour of metal ions in solution one needs to obtain precise information on the interaction between solutes, as well as solute–solvent and solvent–solvent interactions.[1] The determination of the hydration structure of different cations in solution has been the subject of numerous studies in the last two decades. Although most of them were carried out by means of both X-ray and neutron diffraction,[2, 3] special attention has been recently given to the use of extended X-ray absorption fine structure (EXAFS) spectroscopy,[4] because it can provide information on the hydration structure in dilute and even highly dilute solutions.[5]

[a] Dr. J. Chaboy
Insitituto de Ciencia de Materiales de Aragón,
CSIC-Universidad de Zaragoza, 50009 Zaragoza (Spain)
Fax: (+34) 976-761229
E-mail: jchaboy@posta.unizar.es

[b] Dr. A. Muñoz-Páez
Instituto de Ciencia de Materiales-Departamento
de Química Inorgánica, CSIC-Universidad de Sevilla
c/Americo Vespucio s/n, 41092-Seville (Spain)

[c] Dr. S. Díaz-Moreno
European Synchrotron Radiation Facility
Polygone Scientifique L. Neel, 6 rue Jules Horowitz
38100 Grenoble cedex (France)

Beyond its unique characteristics as a structural tool, the increasing interest in EXAFS is linked to the generalisation of user-friendly computer codes to perform the analysis of the EXAFS signals. The determination of reliable structural parameters from EXAFS requires knowledge of backscattering amplitudes and phase shifts that are nowadays easily accessible because of the significant developments in the theoretical models. This progress has developed into the creation of new computer codes with robust modelling capabilities to fit EXAFS data by the use of theoretical standards.[6] However, most of the present models and associated codes are built into a framework based on the one-electron theory. Hence, despite the attained improvements, these codes cannot account for features in the EXAFS signal that result from multi-electron processes.

Multi-electron excitations, in which two or more electrons are simultaneously excited, can contribute to the EXAFS spectra and thus influence the obtained structural information. The relevance of these findings for EXAFS data analysis has motivated a large body of both experimental and theoretical research.[7–9] In particular, exhaustive studies have been carried out on lanthanide-based materials in order to make clear the influence of multiple-electron transitions on the EXAFS signals at the rare-earth L- absorption edges.[10] In these studies it was concluded that multi-electron excitations induce additional features in the EXAFS signal far above the edge, and result in the worsening of the usual precision claimed for the EXAFS technique (i.e., 10% for coordination

0947-6539/01/0705-1102 $ 17.50+.50/0

numbers and 0.01 Å for interatomic distances). Moreover, what is also demonstrated with regard to the L-edges of rare-earth compounds is that the effect of multi-electron excitations in EXAFS is not negligible, even in crystalline systems.[8, 10] This result is noteworthy because traditionally multi-electron transitions have been readily identified only in disordered systems, in which the intensity associated with these excitations is comparable with the amplitude of the EXAFS oscillation.[11, 12]

In the light of the influence of multi-electron processes on the EXAFS analysis, it would be interesting to extend the study of this interplay to solutions of metal complexes. Indeed, we recently performed a detailed EXAFS study of aqueous solutions of $YBr_3 \cdot 6H_2O$ (0.005–2.0 molal) in liquid and glassy states to determine the solvation structure of the yttrium(III) cation in dilute and concentrated aqueous solutions. The EXAFS analysis indicates both the existence of a symmetric polyhedron of water molecules around the yttrium(III) cations at 2.35 Å and the absence of contact Y–Br ion pairs in all the investigated solutions. However, it was not possible to discern from the EXAFS analysis whether the coordination number with the nearest neighbours was eight or nine. At that stage of the investigation it was proposed that the inaccuracy of the derived coordination number was related to the existence of a multi-electron transition within the EXAFS regime.[13] In order to gain a deeper insight into this problem, we have systematically investigated the presence of multi-electron features on the Y K-edge EXAFS spectra of several solutions and solid compounds of yttrium(III) cations. For the sake of completeness we have also investigated the presence of such multi-electron features at the Br K-edge EXAFS in solid YBr_3 and its solutions.

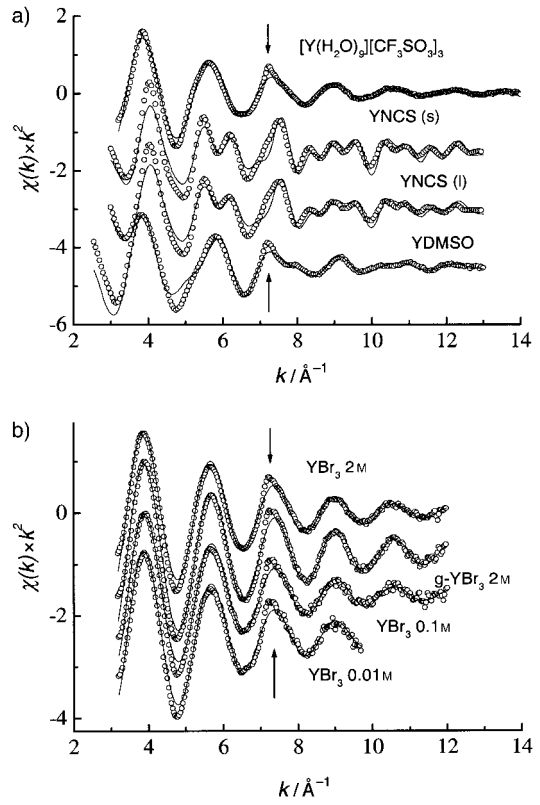

Figure 1. Comparison between the experimental (○) and theoretically calculated (——) Y K-edge $\chi(k)\cdot k^2$ EXAFS signals for the different compounds under investigation: a) $[Y(H_2O)_9][CF_3SO_3]_3$, YNCS (liquid and solid) and YDMSO; b) aqueous solutions of $YBr_3 \cdot 6H_2O$, of concentrations 2.0M, 0.1M and 0.01M, as well as glassy g-YBr_3.

Results and Discussion

X-ray absorption experiments at the yttrium K-edge were carried out on i) aqueous solutions (2.0, 0.1 and 0.01M) of yttrium(III) bromide hexahydrate ($YBr_3 \cdot 6H_2O$), ii) solid enneahydrated yttrium(III) trifluoromethanesulfonate $[Y(H_2O)_9][CF_3SO_3]_3$ (hereafter abbreviated as yttrium(III) triflate); iii) solid tetra-*n*-butylammonium hexakis(thiocyanato-*N*)yttrate(III), $[Bu_4N]_3[Y(NCS)_6]$ (henceforth YNCS), and its 0.5M solution in acetonitrile and iv) solid tetrakis(dimethylsulfoxide)yttrium(III) nitrate (YDMSO). In addition, a glassy sample of the YBr_3 2.0M solution (hereafter abbreviated as g-YBr_3) was also investigated. X-ray absorption experiments at the Br K-edge were performed on solid $KBrO_3$ and solutions of $YBr_3 \cdot 6H_2O$.

Figure 1 shows the comparison between the experimental k^2-squared EXAFS signals ($\chi(k)\cdot k^2$) of the various compounds and their theoretical simulations.[13, 15] In the case of the reference compound $[Y(H_2O)_9][CF_3SO_3]_3$, this comparison is fairly satisfactory. Indeed, the fine structure is in good agreement with the calculation except for the region between 7 and 7.5 Å^{-1}. While the experimental EXAFS shows a peak-like feature in this region, the calculation yields a typical EXAFS oscillation. This discrepancy is also detected, at the same energy, in the Y K-edge EXAFS spectra of both liquid and solid YNCS, as well as in the YDMSO sample. Whereas the EXAFS spectrum of the yttrium(III) triflate is quite smooth, this is not the case for YNCS or YDMSO (Figure 1a). The EXAFS spectra of the latter samples contain many absorption features, which indicate a more complex structural environment around the absorbing yttrium atom. Despite the fact that the local structure is quite different in these compounds, all the EXAFS spectra exhibit the same class of discrepancy between the experimental and calculated signals at $\approx$7.2 Å^{-1}. This trend is a first indication of the atomic nature of this peak-like structure, that is, it is not linked to the particular local environment of yttrium but to some absorption process characteristic of the Y K-edge excitation. A similar conclusion can be obtained from inspection of Figure 1b, in which a comparison between the experimental and calculated EXAFS spectra of different concentrations of aqueous solutions of $YBr_3 \cdot 6H_2O$ is shown. For comparative purposes, we have also included the results obtained for the glassy g-YBr_3 sample. In all cases, the EXAFS spectra of YBr_3 solutions exhibit a huge decrease in the fine structure as compared to those of YDMSO and YNCS compounds. Indeed, modulation of their EXAFS signals fits well with a single frequency, in agreement with the existence of a symmetric polyhedron of water molecules around yttrium(III) cations at 2.35 Å.[13] Because the quality of the fit is remarkable, it is simple to detect the same class of anomaly at 7.2 Å^{-1}, as observed in the EXAFS spectra given in

Figure 1a. This discrepancy appears in all the spectra, independent of the concentration, as well as in the glassy sample. These results are summarised in Figure 2, in which the

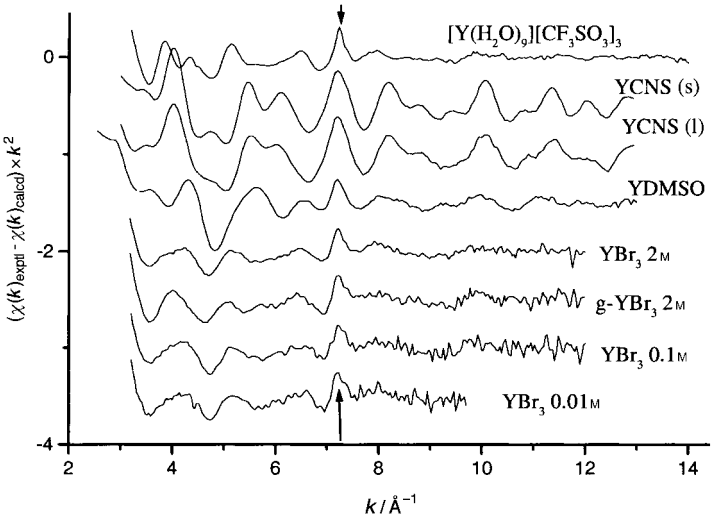

Figure 2. Difference between the experimental Y K-edge $\chi(k)\cdot k^2$ EXAFS signals and their ab-initio calculations given in Figure 1. The arrow indicates the residual spectral feature common to all the investigated compounds.

difference between the experimental EXAFS signals and their corresponding theoretical calculations are shown for all the investigated compounds. In all cases, this comparison clearly shows the presence of a peak whose maximum lies at 7.2 $Å^{-1}$. Hence, independent of the local environment of yttrium (9, 8 and 6 nearest neighbours) and the aggregation state (solid, liquid and glassy), all the Y K-edge EXAFS spectra show an additional feature that cannot be accounted for by the standard one-electron description of EXAFS. On the contrary, we suggest that this effect is caused by a multi-electron transition of non-negligible intensity within the EXAFS region of the spectra.

To verify this possibility and to assess the importance of double-electron excitation channels relative to the main single-electron $1s \rightarrow \varepsilon p$ channel at the Y K-edge in a quantitative manner, we have computed the intensities of the double-electron resonance strengths relative to the main line (single-electron) strengths. The computations were based on a many-body perturbation model for atomic excitation which explicitly includes final state relaxation. A complete description of the model and the calculation method can be found in refs. [8–10]. The results of the calculation for the Y K-edge in are given in Table 1. We have determined the different double-electron transitions expected to occur within the EXAFS regime. The calculation also provides the position of the features associated with the multi-electron process and its intensity, both of them relative to those of the single-electron excitation line, that is, to the white line at the absorption edge. It should be noted that standard EXAFS analyses are performed in the *k*-space, so that is necessary to choose a zero energy. Typically the onset energy is fixed at the maximum of the first derivative in the threshold region, whereas the double-electron energy positions have been

Table 1. Calculated double-electron transition intensities and excitation energies for Y. The position of the double-electron (d.e.) feature is given above the main line (ΔE) and in *k*-space. σ(d.e.)/σ(s.e.) is the ratio of double-electron line-strength to that of the single-electron (s.e.) (in %).

Transition	ΔE[eV]	k[$Å^{-1}$]	σ(d.e.)/σ(s.e.)[%]
1s4p → 5p5p	33.6	3.3	4.68
1s4s → 5p5s	49.71	3.9	1.01
1s3d → 5p4d	185.12	7.14	2.07
1s3p → 5p5p	323.86	9.33	7.15×10^{-2}
1s3s → 5p5s	389	10.2	2.27×10^{-2}

determined with respect to the absorption maximum at the edge. To avoid confusion, Table 1 includes the corresponding *k* values as obtained in a standard EXAFS analysis framework.

From inspection of the results in Table 1, we found that two transitions (1s4p → 5p5p and 1s4s → 5p5s) are predicted to occur at energies close to the edge, that is within the X-ray absorption near-edge spectroscopy (XANES) regime. However, we find that three different double-electron processes are expected to occur in the EXAFS regime. All of them correspond to the excitation of an additional electron from the M level (3s, 3p and 3d) concomitant to the creation of the core-hole in the K shell. However, the strength of these transitions is rather weak. The calculated intensity only appeared to be significant in the case of the 1s3d → 5p4d ($KM_{4,5}$) transition. The comparison between the calculated double-electron signals and the experimental EXAFS spectrum was performed as follows: since the calculation gives the ratio between the single- and double-excitation cross-sections, we determined the intensity of the 1s3d → 5p4d transition from the experimental height of the main white line that corresponds to the 1s → 5p transition. Because the double-electron process corresponds to a transition to the localised p states, we built a Lorentzian function centred at the calculated energy. The height of the Lorentzian is that of the main 1s → 5p transition factorised by the corresponding 2.07×10^{-2} factor (see Table 1). The width of the Lorentzian, Γ, is related to the core-hole lifetime for the considered $KM_{4,5}$ transition. Thus, we have determined Γ to be that of the main 1s → 5p transition, estimated from the full width at half maxiumum height (FWHM) of the white line, and by including the core-hole lifetime that corresponds to the additional 3d excited electron, which is reported to be ≈0.35 eV.[16] As shown in Figure 3a, the white-line intensity is different for the various compounds. Consequently, the double-electron feature is expected to appear with a different intensity on the Y K-edge EXAFS spectra of the different yttrium-based compounds. For example, according to Figure 3a it is expected to be more intense in the case of yttrium triflate than for the YBr_3 solutions.

The so-obtained double-electron features have been plotted in Figure 3b versus the difference between the experimental EXAFS signals and their theoretical fits for several selected cases. The agreement between our calculation and the experimental observations is outstanding and supports our initial assignment to the absorption feature that appears at 7.2 $Å^{-1}$ on the Y K-edge EXAFS spectra. The anomalous

0947-6539/01/0705-1104 $ 17.50+.50/0 *Chem. Eur. J.* **2001**, *7*, No. 5

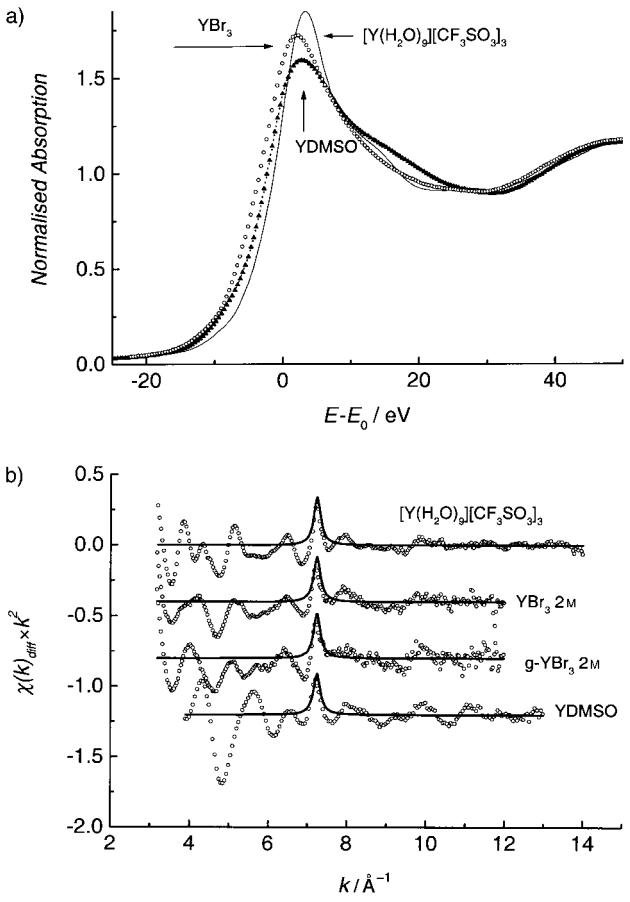

Figure 3. a) Detailed view of the near-edge region of the Y K-edge X-ray absorption spectra for several selected compounds: yttrium(III) triflate (——), 2.0 M $YBr_3 \cdot 6H_2O$ aqueous solution (○), and solid YDMSO (▲). b) Comparison between the calculated 1s3d → 5p4d double-electron signals and the difference between the Y K-edge $\chi(k) \cdot k^2$ EXAFS signals and their ab-initio calculations given in Figure 2 for the selected compounds.

behaviour of the EXAFS resonance centred at 7.2 $Å^{-1}$ is fully reproduced by taking account of the theoretical calculation for the $KM_{4,5}$-edges multi-electron transition. This is shown in Figure 4 in which the experimental EXAFS spectra at the Y K-edge for yttrium triflate is compared to its single-electron theoretical calculation[13, 15] in the region in which the double excitation feature has been identified. The calculated 1s3d → 5p4d multi-electron contribution has been included above the experimental signal. Subsequently, we subtracted the double-electron resonance from the experimental spectrum as shown in Figure 4. The agreement between the calculated energy position and intensity of the double-electron feature and the experimental one can be considered to be very good. The presence of such multi-electron processes introduces an error in the estimation of the coordination number; this is estimated to be ≈5% in the case of solid yttrium(III) triflate, while in the case of 2.0 M $YBr_3 \cdot 6H_2O$ aqueous solution the error reaches ≈12%.[13]

Finally, we studied the Br K-edge. Several reports have been published regarding the presence of multi-electron excitations in the Br K-edge EXAFS region,[17–19] although no unique picture has been obtained. For example, Li et al.[17] and D'Angelo et al.[18] have identified several contributions of double-electron excitation channels to the atomic absorption background. However, while Li and co-workers only identified the $KM_{4,5}$ transition in RbBr, D'Angelo and co-workers have detected the KN_1, $KM_{4,5}$ and $KM_{2,3}$ transitions in both HBr and Br_2. None of them were able to identify the KM_1 transition that is expected to occur close the $KM_{4,5}$ and $KM_{2,3}$ transitions. In both cases, the agreement between the energy position of the multi-electron feature and theoretical estimates differs for the different transitions. In addition, Ito et al. have also identified the $KM_{4,5}$ and $KM_{2,3}$ transitions in a solution of $EuBr_3$ in ethanol (0.01 M);[19] however, they also claim the presence of three-electron transitions. Consequently, the experimental scenery for the existence of these multi-electron excitations on the Br K-edge EXAFS spectra is still unsolved. More important, when comparing previous work[17–19] one finds a large dispersion with regard to the energy position of such multi-electron features on the EXAFS, this being the most important parameter to determine prior to the begin of an EXAFS analysis. Furthermore, no direct determination of the intensity of the multi-electron transitions have been provided, although Li et al. suggest, by comparison with the Kr case, that the amplitude of the Br $KM_{4,5}$ double-excitation is 10^3 times smaller than that of the primary channel. This estimate indicates that the impact of these multi-electron transitions on the EXAFS should be negligible. Indeed, the determination of the interatomic distance in the Br_2 molecule is 2.286 Å after subtraction of the multi-electron contribution[18] and 2.280 Å according to a standard ab-initio EXAFS analysis.[20]

In an effort to gain a deeper insight into the appearance of multi-electron excitation features on the Br K-edge EXAFS, we performed explicit calculations of both the energy position and the intensity of the double-electron 1s3d → 4p4d, 1s3p → 4p5p and 1s3s → 4p5s transitions ($KM_{4,5}$, $KM_{2,3}$ and KM_1) that are expected to occur within the EXAFS regime. The results of this calculation are given in Table 2. Compared to the case of the Y K-edge, the predicted intensities for the multi-electron processes at the Br K-edge are very weak. Indeed, our estimate is that they are one order of magnitude smaller than those of the Y K-edge and, consequently, we do not expect them to have a significant effect on the EXAFS signal. We have experimentally tested these results on solid $KBrO_3$ and an aqueous solution of Ybr_3 (2.0 M). The normalised spectra of the Br K-edge in both samples are shown in Figure 5a. It should be noted that the height of the white-line for $KBrO_3$ is twice that of the YBr_3 solution. Consequently, we expect a clearly different influence of the

Table 2. Calculated double-electron transition intensities and excitation energies for Br. The position of the multiple-electron (m.e.) feature is given above the main line (ΔE) and in k-space. σ(m.e.)/σ(s.e.) is the ratio of multiple-electron line-strength to that of the single-electron (s.e.) (in %).

Transition	ΔE [eV]	k [$Å^{-1}$]	σ(m.e.)/σ(s.e.) [%]
1s3d → 4p4d	95.2	5	3.55×10^{-3}
1s3p → 4p5p	202.75	7.3	1.38×10^{-3}
1s3s → 4p5s	257.73	8.22	4.55×10^{-4}

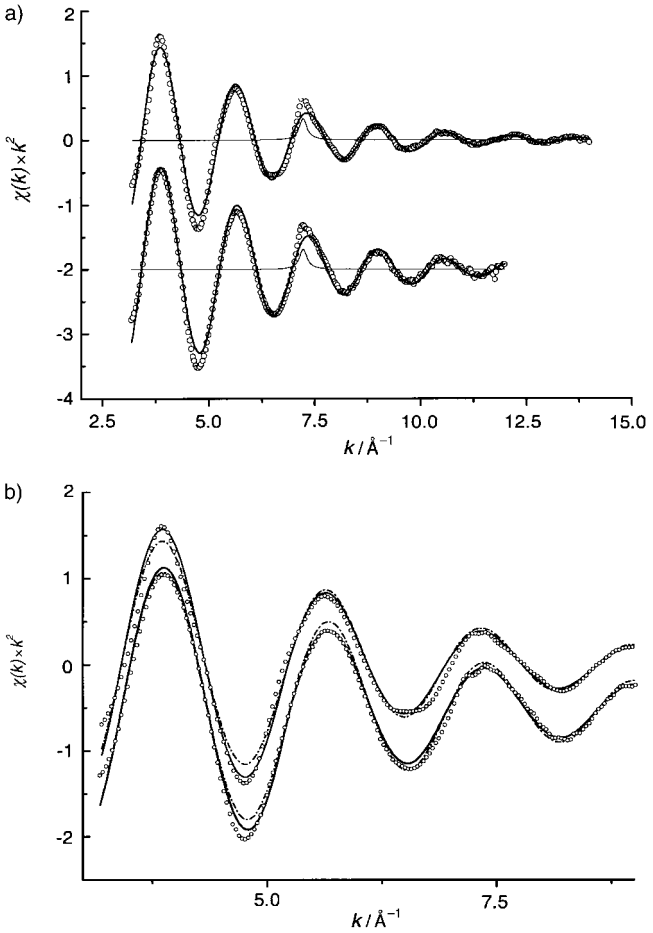

Figure 4. a) Comparison between the experimental Y K-edge $\chi(k)\cdot k^2$ EXAFS signal (○) and its best-fit (——) before subtraction of the multi-electron transition for yttrium(III) triflate (top) and 2.0 M $YBr_3\cdot 6H_2O$ aqueous solution (bottom). The calculated Y $KM_{4,5}$-edge (1s3d → 5p4d) double-electron spectral feature is also shown. b) Comparison between the experimental Y K-edge $\chi(k)\cdot k^2$ EXAFS signal after the subtraction of the Y $KM_{4,5}$-edge and its best-fits before (•–•–) and after (——) subtraction of the multi-electron transition for yttrium(III) triflate (top) and 2.0 M $YBr_3\cdot 6H_2O$ aqueous solution (bottom).

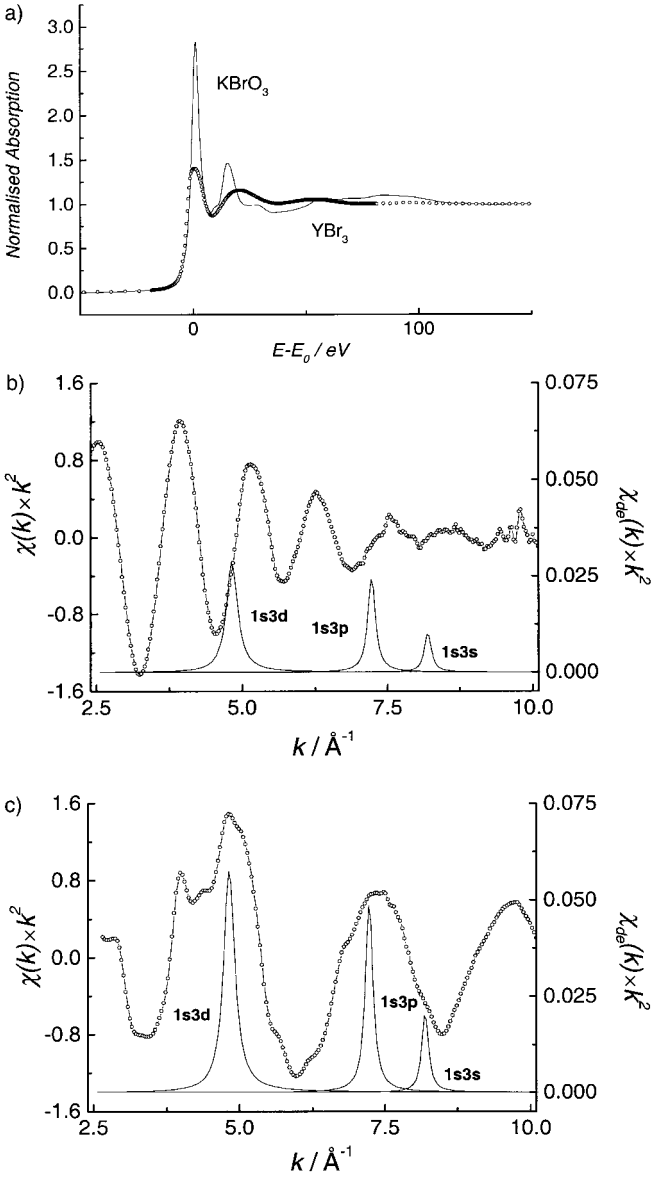

Figure 5. a) Br K-edge X-ray absorption spectra of solid $KBrO_3$ (——) and 2.0 M YBr_3 aqueous solution (○). b) Experimental Br K-edge $\chi(k)\cdot k^2$ signal of $KBrO_3$ (○) and the theoretical $\chi_{d.e.}(k)\cdot k^2$ contribution predicted for the double-electron 1s3d → 4p4d (1s3d), 1s3p → 4p5p (1s3p) and 1s3s → 4p5s (1s3s) transitions. Note that the scale for $\chi_{d.e.}(k)\cdot k^2$ is 40 times smaller than that of the experimental $\chi(k)\cdot k^2$. c) Same kind of comparison as in (b) for 2.0 M YBr_3 aqueous solution.

double-electron processes for both the solid compound and the solution. According to our calculations, the most intense feature is predicted to occur for the $KM_{4,5}$ transition at ≈5 Å, being of similar intensity to the $KM_{2,3}$ transition (≈7.3 Å). The intensity of the KM_1 transition (≈8.2 Å) is estimated to be one order of magnitude smaller.

A comparison between the calculated double-electron signals and the experimental EXAFS spectrum was performed as for the Y K-edge. The results of the comparison are shown in Figures 5b and 5c for $KBrO_3$ and YBr_3, respectively. In the case of $KBrO_3$, the predicted contribution of the studied double-electron processes fits well to several weak modulations of the EXAFS signals. Furthermore, the predicted intensity is in agreement with the experimental situation; while the $KM_{4,5}$ edge seems to give rise to a peak-like contribution superimposed on the Br K-edge EXAFS, it is weaker for the $KM_{2,3}$ channel and finally for the KM_1 transition only a small bump of the main EXAFS oscillation can be detected. These results are in contrast to those obtained for the EXAFS signal of the YBr_3 solution, shown in Figure 5c, in which no hint of any features that result from this multi-electron transition is detected over the signal-to-noise ratio. The absence of a double-electron contribution in this case is in agreement with our prediction as it is a direct consequence of the white-line weakness in the Br K-edge spectrum of the YBr_3 solution that determines the strength for double-electron processes to be at least one order of magnitude smaller than in the case of the $KBrO_3$ compound.

Conclusions

We have identified the presence of an anomalous feature in the Y K-edge EXAFS spectra of different yttrium-based

0947-6539/01/0705-1106 $ 17.50+.50/0 *Chem. Eur. J.* **2001**, *7*, No. 5

compounds. The presence of this resonance, centred at 7.2 Å^{-1}, in the EXAFS signals is independent of the differing local environments of the absorbing atom. This behaviour is caused by a double-electron 1s3d → 5p4d ($KM_{4,5}$)-edge transition. This multi-electron transition is fully accounted for in theoretical calculations based on a many-body perturbation model for atomic excitation, which explicitly includes final state relaxation. These computations provide both the intensity and the position of the multi-electron features on the EXAFS spectra relative to the main excitation line. Thus, it is possible to estimate the effect of these double-electron features on the structural signal at the first level and then subtract them if necessary.

The same class of calculations was also performed for the Br K-edge. Contrary to the Y K-edge case, the results indicated that the effect of double-electron processes in the Br K-edge EXAFS regime is negligible, which is in agreement with the experimental results.

Experimental Section

Yttrium and Br K-edge EXAFS spectra were recorded at the BL10B station of the Photon Factory (National Laboratory for High Energy Physics KEK, Japan). The storage ring was operated at 2.5 GeV, with a stored current of 300 mA. Measurements were performed at room temperature in the transmission mode with a Si(311) channel-cut monochromator and detection ion chambers. The chambers were filled with a flowing gas mixture optimised for each energy. The solid compound yttrium(III) triflate was measured in a sample holder covered by kapton and placed in a hermetically sealed plastic bag, as this sample is very hygroscopic. The non-hygroscopic samples were measured in air, with the exception of the glassy g-YBr_3 sample which was measured at 77 K in a vacuum cryostat. All the liquid samples were measured in a specially designed cell, allowing for variable path lengths.

The EXAFS signals were extracted from the raw absorption spectra by the following standard procedures.[22, 23] In all cases the onset energy of the absorption process was chosen to be the maximum of the first derivative in the edge region of the absorption spectrum. EXAFS data analysis for the $YBr_3 \cdot 6H_2O$ samples, in liquid and glassy states, and for the yttrium triflate, was carried out with the XDAP program[24] with theoretical phase shifts and backscattering amplitudes determined from the FEFF 7.02.[25] Errors in the structural parameters and the quality of the fit was assessed according to the recommendations of the "Standards and criteria for EXAFS data analysis".[26] For the remaining samples, the spectra were calculated with FEFF 6.01 , which takes into account multiple scattering contributions. We limit ourselves here to the discussion of the breakdown of the single-electron approximation in the case of the Y K-edge experimental EXAFS spectra. The detailed EXAFS data analysis have already been published.[13, 15]

Sample preparation:

Yttrium(III) bromide hexahydrate ($YBr_3 \cdot 6H_2O$): The solid hexahydrate was prepared from commercial Y_2O_3 (99.99 % Aldrich) through dissolution in a minimum volume of 48 % HBr. The solution was then evaporated in a sand bath until crystallisation occurred. The white crystals were then separated on a sintered glass filter, and were kept in a desiccator over Al_2O_3. Aqueous solutions of concentrations 2.0, 1.0, 0.5, 0.1, 0.05, 0.01 and 0.005 M were prepared from this compound. In order to avoid hydrolysis of the samples, which could lead to the appearance of other species in solution such as $[Y(OH)(H_2O)_n]^{2+}$, the pH of all the solutions was kept constant at pH = 1.0 by addition of the required amount of $HClO_4$. To study the formation of ion pair structures, aqueous solutions with a ratio Y:Br of 1:6 and 1:9 were prepared by adding NaBr salt to the 0.1 M YBr_3 aqueous solution. A glassy sample of a solution of YBr_3 (2.0 M; g-YBr_3) was prepared by quick immersion of the corresponding aqueous solution into liquid nitrogen and it was then kept at this temperature in a vacuum cryostat. A detailed description of the sample preparation can be found in Refs. [13–15, 21].

Yttrium(III) trifluoromethanesulfonate enneahydrate ($[Y(H_2O)_9][CF_3SO_3]_3$, Y^{3+} triflate): This was also prepared following the method proposed by Harrowfield et al.[27] The solid was used as a model compound against which comparisons could be made since its hydration structure is well known.

$[Bu_4N]_3[Y(NCS)_6]$ (YNCS): Synthesized by deposition in crystalline form from a solution of YCl_3 and tetra-*n*-butylammonium thiocyanate in a molar ratio 1:10 in ethanol.[28] It is soluble in several organic solvents, such as acetonitrile, and partially decomposes in water, by replacement of some SCN^- ligands by water molecules.

$[Y(DMSO)_3](NO_3)_3$ (YDMSO): Excess DMSO (3 mL) was added dropwise with stirring to a solution of yttrium nitrate pentahydrate (≈1 mol) in methanol (15 mL). The solvent was evaporated under reduced pressure over P_2O_5, and a precipitate of the complex was obtained in good yield. The precipitate was filtered, washed with benzene, dried over P_2O_5 and recrystallized from methanol.

Acknowledgements

This work was partially supported by Spanish grants DGICYT MAT99-0667-C04-04 and PB98-1153. We are grateful to the Photon Factory of the Institute of Material Structure Science Project (Project no. 95-G215) at KEK, Tsukuba (Japan) for the allocation of beam-time.

[1] D. T. Richens, *The Chemistry of Aqua Ions*, Wiley, Chichester, **1997**.
[2] Y. Marcus, *Ion Solvation*, Wiley, Chichester, **1986**.
[3] H. Ohtaki, H. Yamatera, *Structure and Dynamics of Solutions*, Elsevier, Amsterdam, **1992**.
[4] P. A. Lee, P. H. Citrin, P. Eisenberger, B. M. Kincaid, *Rev. Mod. Phys.* **1981**, *53*, 769–806.
[5] H. Ohtaki, T. Radnai, *Chem. Rev.* **1993**, *93*, 1157–1204.
[6] Catalogues of X-ray absorption spectroscopy analysis programs can be found on the web pages of the European Synchrotron Radiation Facility (http://www.esrf.fr/computing/scientific/exafs) and the International XAFS Society (http://ixs.csrii.iit.edu/IXS/catalog/XAFS Programs/).
[7] A. Filipponi, *Physica B* **1995**, *208 & 209*, 29–32.
[8] J. Chaboy, T. A. Tyson, *Phys. Rev. B* **1994**, *49*, 5869–5875.
[9] J. Chaboy, A. Marcelli, T. A. Tyson, *Phys. Rev. B* **1994**, *49*, 11652–11661.
[10] J. Chaboy, A. Marcelli, T. A. Tyson, *Relative Cross Sections for Bound-State Double-Electron $LN_{4,5}$-Edge Transitions of Rare Earths and Nonradiactive Elements of the Sixth Row*, Prensas Universitarias de Zaragoza, Saragossa (Spain), **1995**.
[11] J. Chaboy, J. García, A. Marcelli, M. F. Ruiz-López, *Chem. Phys. Lett.* **1990**, *174*, 389–395.
[12] S. Stizza, M. Marziali, O. Gzowski, J. Chaboy, A. Marcelli, K. Szaniawska, *Jap. J. Appl. Phys.* **1993**, *Suppl. 32–2*, 797–799.
[13] S. Díaz-Moreno, A. Muñoz-Páez, J. Chaboy, *J. Phys. Chem. A* **2000**, *104*, 1278–1286.
[14] S. Díaz-Moreno, J. M. Martínez, A. Muñoz-Páez, H. Sakane, I. Watanabe, *J. Phys. Chem. A* **1998**, *102*, 7435–7441.
[15] S. Díaz-Moreno, Ph. D. Thesis, Seville University (Spain), **1998**.
[16] K. D. Sevier, *Low Energy Electron Spectrometry*, Wiley Interscience, New York, **1972**, Chapter 6.
[17] G. Li, F. Bridges, G. S. Brown, *Phys. Rev. Lett.* **1992**, *68*, 1609–1612.
[18] a) P. D'Angelo, A. Di Cicco, A. Filipponi, N. V. Pavel, *Phys. Rev. A* **1993**, *47*, 2055–2063; b) E. Burattini, P. D'Angelo, A. Di Cicco, A. Filipponi, N. V. Pavel, *J. Phys. Chem.* **1993**, *97*, 5486–5494.
[19] Y. Ito, T. Mukoyama, S. Emura, M. Takahashi, S. Yoshikado, K. Omote, *Phys. Rev. A* **1995**, *51*, 303–308.
[20] J. Mustre de León, J. J. Rehr, S. I. Zabinsky, R. C. Albers, *Phys. Rev. B* **1991**, *44*, 4146–4156.
[21] S. K. Ramalingam, S. Soundararajan, *J. Inorg. Nucl. Chem.* **1967**, *29*, 1763–1768.

[22] See, for example: D. E. Sayers in *X-ray Absorption: Principles, Applications, Techniques of EXAFS, SEXAFS and XANES* (Eds.: D. C. Koningsberger, R. Prins), John Wiley & Sons, New York, **1988**, Chapter 6.
[23] B. Lengeler, P. Eisenberger, *Phys. Rev. B* **1980**, *21*, 4507 – 4519.
[24] M. Vaarkamp, J. C. Linders, D. C. Koningsberger, *Physica B* **1995**, *208 & 209*, 159 – 160.
[25] S. I. Zabinsky, J. J. Rehr, A. Ankudinov, R. C. Albers, M. J. Eller, *Phys. Rev. B* **1995**, *52*, 2995 – 3009.
[26] F. W. Lytle, D. E. Sayers, E. A. Stern, *Physica B* **1989**, *158*, 701 – 722.
[27] J. M. Harrowfield, D. L. Kepert, J. M. Patrick, A. H. White, *Aust. J. Chem*. **1983**, *36*, 483.
[28] S. K. Ramalingam, S. Soundararajan, *J. Inorg. Nucl. Chem*. **1967**, *29*, 1763 – 1768.

Received: June 21, 2000 [F2558]

  0947-6539/01/0705-1108 $ 17.50+.50/0